HIGH SPEED ALGORITHMS FOR THE FULL PENETRATION HOLE DETECTION IN LASER BEAM WELDING PROCESSES BY CELLULAR NEURAL NETWORKS

Leonardo Nicolosi
Technische Universität Dresden
Dresden, Germany
leonardo.nicolosi@tu-dresden.de

Ronald Tetzlaff
Technische Universität Dresden
Dresden, Germany
ronald.tetzlaff@tu-dresden.de

Abstract

New visual algorithms for the control of keyhole welding processes are proposed in this paper. Keyhole welding allows obtaining highly focused laser beam, deep and slender weld seams and minimized heat affected zone at high feeding rates. These characteristics make the keyhole welding particularly suitable for several manufacturing processes, from automobile production to precision mechanics. Despite the improvement in welding technology, sophisticated methods of fault detection are not commonly used in commercially available equipments yet. Recent analyses of process images have revealed the possibility to adjust the laser power according to the detection of the so called full penetration hole. Due to the high welding dynamics, rapid physical movements of the full penetration hole can be observed. Therefore, robust closed loop control systems require fast real time image processing with frame rates in the multi kilo Hertz range. In the following, new Cellular Neural Network based strategies for the full penetration hole detection will be proposed. Such algorithms have been implemented in the Eye-RIS system v1.2 and frame rates up to 24 kHz have been reached. The best strategy in precision and time consumption has been already tested in real time applications and some experimental results will be also discussed.

Key words

Cellular Neural Networks, Closed loop systems, Feature extraction, Feedback, Laser welding, System application and experience.

1 Introduction

In the last few decades the laser beam welding (LBW) outclassed older welding techniques in the industrial scenario. The main difference between these strategies is the energetic source used to melt the base material [Fortunato and Ascari, 2008]. The most important characteristic of the laser is the huge power density that the beam can convey on the joining partners. Such energy allows the local vaporization of the metal and the formation of a capillary, conventionally called *keyhole*. The keyhole stays open due to the metal vapor pressure, through which the beam can deeply penetrate and couple its power over the whole surface from the top of the capillary to the bottom. If an opportune laser power is used due to the hydrostatic pressure of the metal vapor, all the plates of the welding setup are penetrated, creating the so called *full penetration*. After the keyhole formation, laser light is transmitted through the hole reducing back reflections to the outside. Keyhole weldings show extreme efficiency since the heat dissipation into the workpiece is really low. Meanwhile the laser beam advances, the fluid material solidifies behind the keyhole creating a deep and slender weld seam.

By the use of this strategy, moreover, high feeding rates up to 50 m/min can be reached. The LBW processes treated in this paper have been executed to join a stack of two steel sheets 0.7 mm thick, with a gap of 0.1 mm. Figure 1 shows a longitudinal section of the materials during the laser welding process and the resulting image of a coaxial process control camera. The latter represents the thermal radiation of the melt in the spectral range of 820 nm to 980 nm. The state of full penetration is visible in the coaxial camera image as a dark zone directly behind the laser interaction zone, the so called *full penetration hole*. It ensures that the two materials are properly connected over the whole cross section after re-solidification and, therefore, it represents an important quality feature which guarantees the strength of the connection.

This paper is focused on the implementation of algorithms on the Eye-RIS system v1.2 [AnaFocus] for the detection of the full penetration hole.

It is a compact and modular vision system which allows sensing and elaborating grey-scale and binarized images. It includes tools for interpreting the information contained in the image flow and for supporting

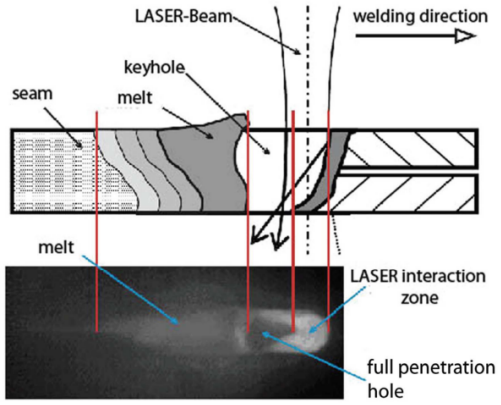

Figure 1. Schematics of a welding process in an overlap-joint and nomenclature. The picture shows on top the longitudinal section of the materials during the welding process and on bottom the resulting image of a coaxial process control camera.

decision-making based on the outcome of such interpretation. The Eye-RIS system consists essentially of an Anafocus' Q-Eye Smart Image Sensor (SIS), an Altera NIOS II processor and I/O ports.

The Q-Eye is a quarter CIF resolution fully programmable smart image sensor. It consists of 176 x 144 cells, each containing a processor merged with an optical sensor, memory circuitry and interconnections to the 8 neighboring cells. This means that each pixel can both sense the corresponding spatial sample of the image and process this data in close interaction and cooperation with other pixels. This concept, which has its basis in Cellular Neural Network (CNN) theory [Corinto, Gilli and Civalleri, 2002], is the transition from the Image Sensor (IS) to the SIS.

The Altera NIOS II processor is a FPGA-synthesizable digital microprocessor used to control the operation of the whole vision system and to analyze the information output of the SIS by performing all the decision-making and actuation tasks.

The I/O module includes digital input and output ports, such as SPI, UART, PWM ports, GPIOs and USB 2.0, to interface the Eye-RIS system with external devices.

2 Algorithms

The algorithms discussed in this paper for the full penetration hole detection are based on the method described in [Geese, Tetzlaff, Carl, Blug, Höfler and Abt, 2008] called *ArcFill Algorithm* and implemented in the Eye-RIS system v1.1. The execution of the ArcFill algorithm leads to a single image processing time of about 97 μs. In spite of that, the Eye-RIS system v1.1 is only an experimental prototype and it cannot be used in real applications for several reasons. At first the poor performance of the sensor leads to the introduction of several software operations, in order to improve the quality of the image, slowing the algorithm down. Furthermore, the Eye-RIS system v1.1 does not allow easy interfacing with external devices and this would represent a limit for real time control of welding processes. With the Eye-RIS system v1.2 new important characteristics have been introduced making it faster and more efficient, improving both the sensing and the interfacing phases. For this reason, new strategies for the full penetration hole detection have been studied in order to be applied in the Eye-RIS system v1.2.

2.1 ArcFill Algorithm

The arcFill algorithm was implemented in the Eye-RIS system v1.1. Since the image acquired by this system has not a good quality due to pixelization effects, a preliminary operation is needed. It consists in applying a special thresholding function which performs a 3x3-neighborhood average calculation before binarizing the source image. This allows smoothing the interaction zone edges and leads to better processing results. The subsequent execution of the arcFill template allows dilating the internal edges of the full penetration hole area. In order to extract the filled area, moreover, a logic XOR operation between the thresholded and the filled images is applied. At last, a masking operation is performed in order to cut away most of the noise produced along the external edges of the interaction zone. The flow chart in Figure 2 clarifies the algorithm.

2.2 New strategies

In the following new strategies for the full penetration hole detection implemented in the Eye-RIS system v1.2 will be described. The different programming environment makes the function by function translation of the arcFill algorithm impossible from the old system to the new one. The first attempt, nevertheless, was to reproduce the arcFill algorithm using the available Q-Eye function library. The smoothing threshold and the arcFill template are executed by the convolution function, which slows the algorithm down to about 1033 μs. Besides the extreme image processing time, as shown in Figure 3 (a) the results are not satisfying,

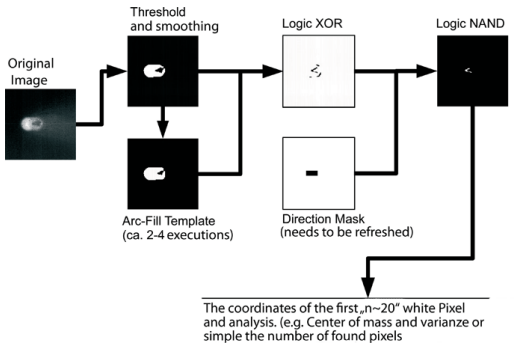

Figure 2. ArcFill algorithm implemented on the EyeRis system v1.1. The flow chart describes the operations performed to detect the full penetration hole.

as the full penetration hole and the surrounding noise have a comparable number of white pixels. Therefore, alternative methods to fill the full penetration hole have been studied. Each algorithm was tested with different kind of images, acquired during real welding processes by the Eye-RIS system. In this paper only results obtained with two typical welding images (one with and one without full penetration hole) will be presented.

2.2.1 ConvexHull algorithm. The second strategy, called *convexHull algorithm* is based on the research in the binarized source image of objects characterized by convex hull boundaries with orientations multiples of 45°. Logical operations come after the execution of the convexHull template in order to extract the filled area. The total time for the elaboration of one single image is estimated around 129 μs. As shown in Figure 3 (b), the full penetration hole can be easily distinguished from the noise due to the elaboration of the interaction zone external edges. Nevertheless, the resulting image presents noise all around the interaction zone and, therefore, it is really complicated to apply accurate masking operations.

2.2.2 ExtractHoles algorithm. The *extractHoles algorithm* is based on an in-built Q-Eye function which allows extracting black objects belonging to a closed white area. The total time consumption for the elaboration of one single image is estimated around 88 μs. Unfortunately, as shown in Figure 3 (c), only few images during the welding process present an interaction zone with a closed white area and, therefore, this strategy cannot be used.

2.2.3 HitAndMiss algorithm. The *hitAndMiss algorithm* is based on iterative pattern researches in the binary image. The pattern is specified as a 3x3 matrix in which each element can be 1 (white), 0 (do not care) or -1 (black) in order to find the internal edges of the full penetration hole. Therefore, after the application of a global threshold value, an iterative pattern research is performed. Since the result of one iteration includes only the filled area, it must be followed by a logic OR with the source image in order to apply the subsequent iteration. The pattern research leads at the end to the extraction of half full penetration hole. The total time for the elaboration of one single image is estimated around 57 μs and the result is shown in Figure 3 (d). The hitAndMiss algorithm was also developed in order to perform two different iterative pattern researches in the binary image in order to extract the whole full penetration hole. The total time for the execution of a double pattern research is around 66 μs per image. The result can be observed in Figure 3 (e).

2.2.4 Dilation algorithm. The last method, called *dilation algorithm*, replaces the iterative pattern research of the hitAndMiss algorithm with dilations toward the image diagonal. A 3x3 pattern allows to specify the direction of the dilation. Since logical ORs after each iteration are not needed anymore, the dilation algorithm is slightly faster than the hitAndMiss algorithm leading to a single image processing time of about 40 μs. This strategy was also developed in order to perform the dilation in two opposite directions with a total time consumption of 52 μs per image. The re-

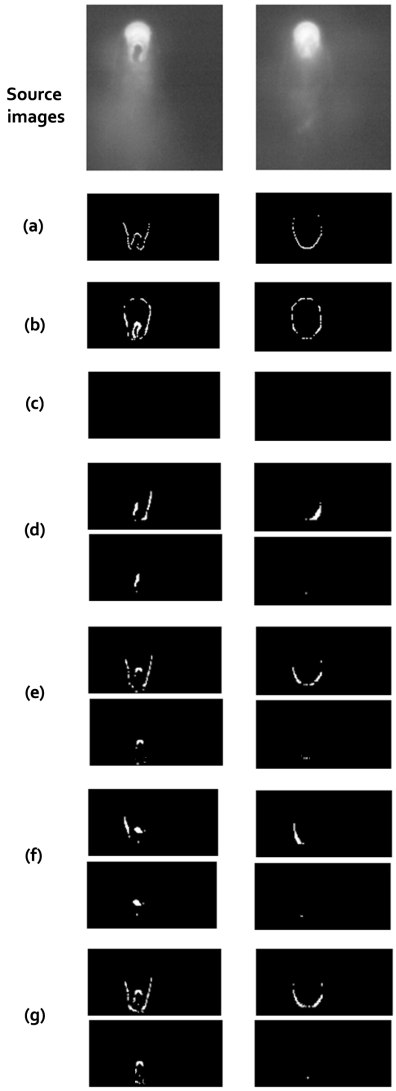

Figure 3. Algorithm results for two source images (with and without full penetration hole). In (a) and (b) the results obtained respectively by the arcFill and the convexHull algorithms are shown. The extractHoles algorithm results, instead, are presented in (c). The full penetration hole, in this case, is not detected because it does not belong to a white closed area. This method, therefore, cannot be used for our purpose. Pictures (d) and (e) are the results obtained performing the hitAndMiss algorithm with one pattern research and two pattern researches respectively. At last (f) and (g) show the results of the 1-side dilation and the 2-sides dilation algorithms respectively. From (d) to (g) both results before and after masking operations are showed. The resulting images have been cut around the interaction zone.

sults obtained by the execution of the former method, called *1-side dilation algorithm*, are shown in Figure 3 (f), while the results obtained by the latter, called *2-sides dilation algorithm* are described in Figure 3 (g).

A detailed explanation of the 1-side algorithm can be found in [Nicolosi, Tetzlaff, Abt, Höfler, Blug, Carl, 2009].

Table 1 sums up the time consumptions of those algorithms previously described which can be used in real time applications.

2.3 Simulation results

According to the results, the dilation and the hitAndMiss algorithms respect the initial request of high frame rate, providing similar results. Since the dilation algorithms are faster, they were used in real time applications. Despite the noise and the full penetration hole have a comparable number of white pixels in the results shown in Figure 3 (d)-(g), it is possible to reduce the noise by masking operations. They are simple to implement as the noise is generated in a known position of the image. Masking operations take an additional time of 2 μs and 18 μs for the 1-side and 2-sides dilation algorithms respectively.

The dilation algorithms were also simulated with several image sequences acquired during real welding processes and hit percentages greater than 88 % were reached, as shown in Table 2.

3 Real time control of welding processes

As described above, the 1-side and the 2-sides algorithms allow the detection of the full penetration hole with a high hit percentage and a high frame rate. Therefore, they have been used for real time control of welding processes. In the past, several authors have proposed closed-loop control systems by using, e.g. the laser power, the focal-point position, or other parameters as the actuator [Bardin, Cobo, Lopez-Higuera, Collin, Aubry, Dubois, Högström, Nylen, Jonsson, Jones, Hand, 2004]. In this paper a feedback strategy by changing the laser power accordingly to the visual detection of the full penetration hole is proposed.

Table 1. Time consumptions of algorithms usable in real time applications.

Algorithm	Time consumption [μs/image]
ArcFill	1024
1-side hitAndMiss	48
2-sides hitAndMiss	57
1-side dilation	40
2-sides dilation	52

Table 2. Dilation algorithm simulation results.

Image sequence	1-side alg	2-sides alg
1	$\approx$ 99 %	$\approx$ 99 %
2	$\approx$ 93 %	$\approx$ 94 %
3	$\approx$ 92 %	$\approx$ 91 %
4	$\approx$ 90 %	$\approx$ 88 %

3.1 Available hardware

In order to obtain a closed loop control of the process, the Eye-RIS system must be connected to the welding machine. The available hardware, therefore, essentially consists of: the Eye-RIS system v1.2, a numerically controlled (NC) machine, the laser and the interface board. The NC machine is responsible for safety interlocks, laser ON/OFF signals and movement. The laser power is controlled by an analog voltage between 0 and 10 V which corresponds to 0-100 % of the laser power. The NC machine sends the starting 24 V digital signal in order to starts the laser and the algorithm flow. Consequently, the machine movement is set in action and the Eye-RIS system begins acquiring and elaborating images and changing the laser power accordingly to the result of the image elaboration in real time. The interface board was built to connect the laser and the NC machine with the Eye-RIS system. Figure 4 shows the real time control algorithm flow chart.

The welding experiments have been carried out with a 2D-laser scanner setup and a constant welding direction. The laser source is a 6 kW, 1030 nm Trumpf

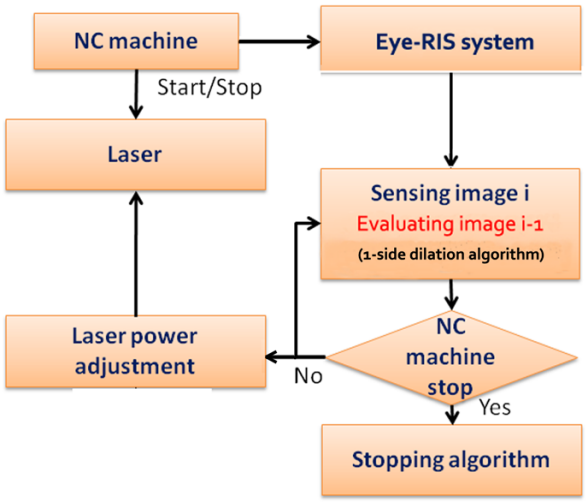

Figure 4. Real time control algorithm flow chart. The numerically controlled (NC) machine sends the signals to begin and stop the algorithm flow. As soon as the start signal is received, the Eye-RIS system starts acquiring and elaborating images. By the 1-side dilation algorithm the full penetration hole can be detected. If the latter is found the laser power is decreased or increased otherwise. One complete control step is performed in about 75 μs.

TruDisk 6002 Yb:YAG thin disk with a 200 μm transport fibre. The laser scanner used - a Trumpf PFO-33 - was equipped with a 450 mm focusing optic which resulted in a focal diameter of 600 μm. The Eye-RIS system is connected to the scanner optic through a 90° beam splitter. Thus the camera perspective is coaxial to the laser beam, providing an invariant field of view regardless of the scanner position. Furthermore. a lens system consisting of three achromatic lenses in combination with an optical band-pass filter was designed to obtain the region of interest (ROI) for the camera. More details can be found in [Abt, Nicolosi, Carl, Blug, Geese, Dausinger, Deininger, Höfler, Tetzlaff].

3.2 Experimental results

In the following typical experimental results will be described. The application of the algorithms leads to frame rates up to 24 kHz. Nevertheless, two additional phases for the real time control must be considered in order to perform sensing and controlling operations. Sensing and image elaboration are simultaneously performed: while the image *i* is being acquired, the image *i-1* is elaborated in parallel. Therefore, the sensing exposure time directly depends on the elaborating time. The sensing phase takes an additional time of about 15 μs. Controlling operations allow changing the laser power accordingly to the processing result and their execution requires an additional time of about 15 μs. One complete control step takes, therefore, about 75 μs and 100 μs for the 1-side algorithm and the 2-sides algorithm respectively, i.e. control frequencies within 10 - 13 kHz can be reached.

In the following two different welding experiments are discussed. The first one regards the joining of two sheets of material with variable thickness, keeping the machine speed constant (4 m/min) during the process. The base material is 1.0 mm thick, while the upper material thickness increases from 0.7 to 1.0 mm in the welding direction. At the beginning, the control system heads the laser power to the first full penetration state. As soon as the thicker material is hit, the full penetration hole is not found in the process image anymore and the control system reacts increasing the laser power until a new stable full penetration state is reached. Figure 5 shows that the system detected the full penetration hole absence by the thickness step and increased opportunely the laser power avoiding full penetration losses.

The second experiment regards the joining of two sheets of material with constant thickness and variable machine speed (from 9 to 3 m/min through 7 and 5 m/min). As shown in Figure 6, the control system changed the laser power accordingly to the feeding rate variation avoiding holes or cuttings due to process decelerations.

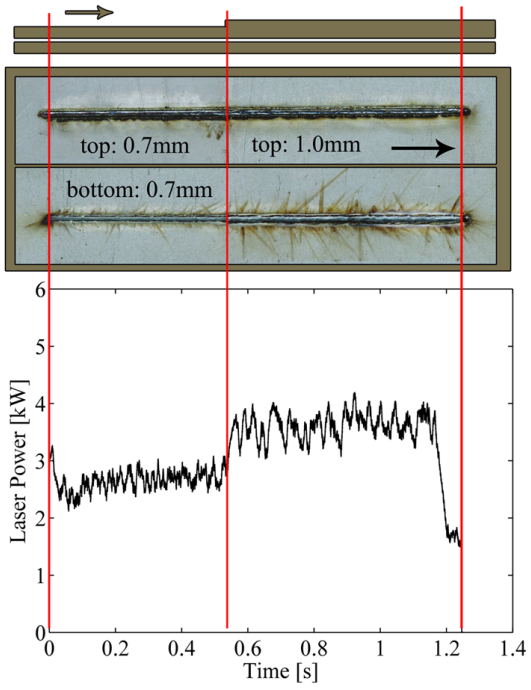

Figure 5. Controlled full penetration weld. Parameters are v = 4 m/min, base material sheet 0.7 mm thick, upper material sheet with variable thickness from 0.7 mm to 1.0 mm in the welding direction. The image at the top shows the welding result, while the image at the bottom shows the controlled laser power response.

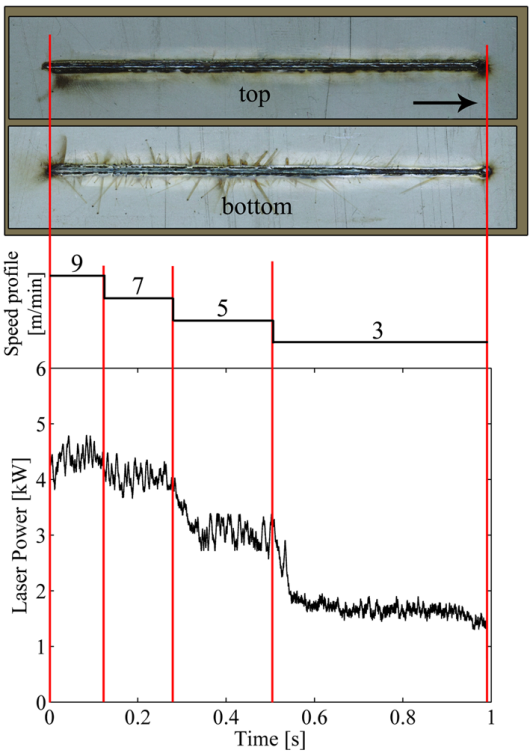

Figure 6. Controlled full penetration weld. Parameters are v = 4 m/min, base material sheet 0.7 mm thick, upper material sheet with variable thickness from 1.0 mm to 0.7 mm in the welding direction. The image at the top shows the welding result, while the image at the bottom shows the controlled laser power response.

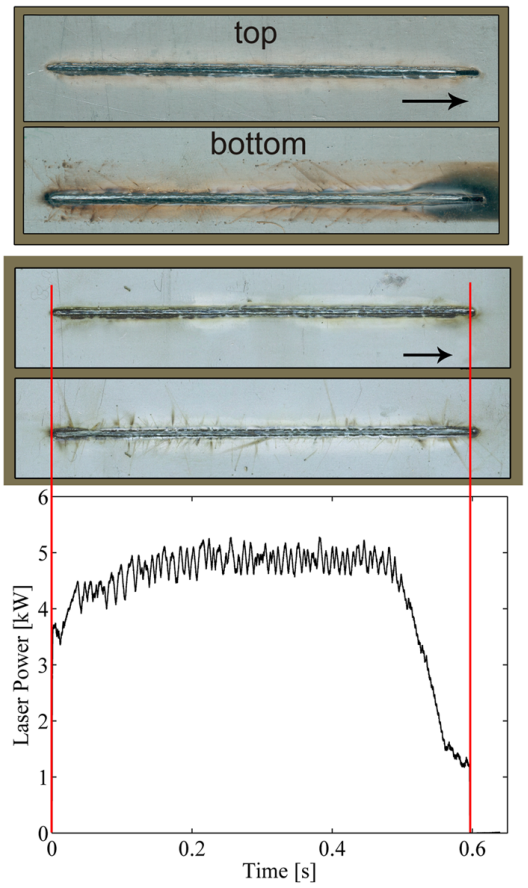

Figure 7. Controlled versus uncontrolled welding of two zinc coated steel sheets 0.7 mm thick with 0.1 mm gap in an overlap joint, with a feeding rate of 9 m/min. The result at the top was obtained by an uncontrolled full penetration weld with constant laser power P = 5.5 kW and 10% laser power as safety factor. The picture at the bottom shows, instead, the controlled full penetration weld. Unlike the latter, the uncontrolled weld result present smoke residue and craters on the bottom side of the joining partners.

The experiments only just discussed are two examples of a vast area of welding processes which can be efficiently controlled by the use of the system proposed in this paper.

4 Conclusion

This paper proposed a new strategy for the real time control of LBW. The full penetration hole was used as image quality feature to build up a closed loop system for the laser power with controlling frequencies up to 13 kHz. The control algorithm was implemented on a CNN based camera system which allows increasing the frame rate by an order of magnitude compared to conventional FPGA based systems. A high frame rate is necessary to improve the robustness of the welding process. As shown in Figure 7, the proposed closed loop system leads to a significant reduction of smoke residue and spatters on the bottom side of the material compared to uncontrolled processes. Furthermore, it introduces the possibility to handle particular welding situations such as variable feeding rate or variable material thickness. Therefore, CNN based architectures have proved their ability to meet the requirements for the real time control of LBW. Nevertheless, the control algorithm presupposes that the welding orientation is kept constant during the process, since it is based on dilations along one specific direction. Further studies have been focusing on the implementation of new orientation-independent strategies.

Acknowledgements

The results showed in this paper have been obtained in the project "Analoge Bildverarbeitung mit zellularen neuronalen Netzen (CNN) zur Regelung laserbasierter Schweißprozesse (ACES)", sponsored by the "Landesstiftung Baden-Württemberg" in the field "Forschung Optische Technologien 2005/2006".

References

Abt F., Nicolosi L., Carl D., Blug A., Geese M., Dausinger F., Deininger C., Höfler H., Tetzlaff R., *Closed Loop Control of Laser Welding Processes with Cellular Neural Network (CNN) Cameras*, Laser Institute of America - LIA - ICALEO 2008, in Proc. of 27th International Congress on Applications of Lasers and Electro Optics, October 20-23 2008, Temecula, CA, USA. Paper 1706.

Company AnaFocus, Avd. Isaac Newton s/n, Pabellón de Italia, Parque Tecnológico Isla de la Cartuja, 41092 Seville, Spain. www.anafocus.com.

Bardin F., Cobo A., Lopez-Higuera J., Collin O., Aubry P., Dubois T., Högström M., Nylen P., Jonsson P., Jones J., Hand D., *Process Control of Laser Keyhole Welding*, in Proc. of the 23rd International Congress on Applications of Lasers and Electro-Optics, ICALEO 2004, San Francisco, USA.

Corinto F., Gilli M. and Civalleri P.P., Dipartimento di Elettronica, Politecnico di Torino, Corso Duca degli Abruzzi 24, I-10129 Torino, Italy, *On stability of full range and polynomial type CNNs*, in Proc. of the 7th IEEE International Workshop on Cellular Neural Networks and their Applications, pp.33-40.

Fortunato, A., Ascari, A. (2008). *Tecnologie di giunzione mediante saldatura. Procedimenti non convenzionali e allo stato solido, Vol.2*, Progetto Leonardo Bologna.

Geese M., Tetzlaff R., Carl D., Blug A., Höfler H. and Abt F., *Feature Extraction in Laser Welding Processes*, in Proc. of the 11th IEEE International Workshop on Cellular Neural Networks and their Applications, CNNA 2008, Santiago de Compostela, Spain.

Nicolosi, L., Tetzlaff R., Abt F., Höfler H., Blug A. and Carl D., *New CNN based algorithms for the full penetration hole extraction in laser welding processes*, in Proc. of the 2009 IEEE International Symposium on Circuits and Systems, ISCAS, pp. 2713-2716, May 24-27, 2009 Taipei, Taiwan.